ChemComm

COMMUNICATION

View Article Online
View Journal | View Issue

Cite this: *Chem. Commun.*, 2015, 51, 10218

Received 22nd April 2015,
Accepted 21st May 2015

DOI: 10.1039/c5cc03323c

www.rsc.org/chemcomm

Peptoid nanosheets as soluble, two-dimensional templates for calcium carbonate mineralization†

Joo Myung V. Jun, M. Virginia P. Altoe, Shaul Aloni and Ronald N. Zuckermann*

Nacre-mimetic materials are of great interest, but difficult to synthesize, because they require the ordering of organic and inorganic materials on several length scales. Here we introduce peptoid nanosheets as a versatile two-dimensional platform to develop nacre mimetic materials. Free-floating zwitterionic nanosheets were mineralized with thin films of amorphous calcium carbonate (of 2–20 nm thickness) on their surface to produce planar nacre synthons. These can serve as tunable building blocks to produce layered brick and mortar nanoarchitectures.

Nature has evolved sophisticated ways to generate materials of extraordinary mechanical strength and toughness from relatively soft components. One of the most outstanding examples is nacre, the iridescent inner layer of abalone shell, which is a hierarchically structured organic–inorganic composite material. Although nacre is composed of ~95% (v/v) calcium carbonate ($CaCO_3$), a relatively fragile mineral, it exhibits extraordinarily high mechanical strength and toughness, of up to 3000 times that of aragonite alone, due to its multi-scale "brick-and-mortar" structure.[1,2] Such remarkable mechanical properties are due to the release of tension through an elastic proteinaceous matrix, which makes up only 5% (v/v) of the entire material.[3,4] The excellent interplay of the inorganic and organic components of nacre provide inspiration for chemists and material scientists to develop lightweight, strong, stiff, and tough materials.[5,6] The ability to emulate nacre-like properties with scalable, synthetic materials promises a new generation of lightweight, tough materials that could benefit sustainability and energy-efficiency in a wide number of industries, including construction, transportation, biomedical implants and shatter-resistant armor.[5] Although layered composite materials of this type are important, there are relatively few methods to synthesize them with a high degree of structural control and on large scales. Therefore, efficient and simple pathways to biomimetic inorganic–organic composite materials are urgently needed.

Nacre is composed of a tiled assembly of $CaCO_3$ (aragonite) plates and acidic protein layers[7] in a brick-and-mortar structure. The intrinsic toughness of nacre is driven by orchestration of the aragonite 'bricks' that are ~0.5 μm thick, 5–10 μm wide, and an organic biopolymer 'mortar' layer[8] (10–50 nm thick) that separates the bricks in-between.[9] The mineral platelets account for the high strength, but are inherently brittle. However, the softer, proteinaceous nanolayers play an important role as a lubricant to allow some movement between the platelets, which results in significantly increased toughness.[9]

Materials chemists have made great recent progress in developing synthetic mimics of nacre. Well-established techniques to produce artificial nacre include supramolecular self-assembly,[8] crystallization on self-assembled monolayers,[10] layer-by-layer (LBL) assembly,[11,12] and freeze-casting.[13] Earlier Sellinger *et al.*[14] developed simple dip-coating and self-assembly process to generate a poly(dodecylmethacrylate)–silica nanocomposite, and Tang *et al.*[15] used a layer by layer method, sequentially depositing cationic polyelectrolyte and montmorillonite clay platelets to produce nacre-mimetic composite materials. Though these systems successfully mimicked the hierarchical structure of nacre, they used non-calcareous inorganic components or an insoluble rigid substrate for mineral growth. One of the recent successful attempts to synthesize nacre-like $CaCO_3$ multilayers[16] used polymer mediated mineral growth followed by the layer-by-layer deposition of porous organic films. However, the LBL process has practical limitations, as it needs many repetitive steps to build thick multilayers, and requires removal of the templating substrate to produce free-standing nanostructured materials.[17,18] Thus it remains a challenge to produce such materials on a large scale and in high yield. To our knowledge, no $CaCO_3$ thin films have been produced in solution on free-floating soluble organic planar templates. Herein, we introduce a new self-assembling, structurally well-defined organic planar matrix that is readily surface functionalized and optimized for $CaCO_3$ mineralization in solution.

The Molecular Foundry, Lawrence Berkeley National Laboratory, 1 Cyclotron Road, Berkeley, CA 94720, USA. E-mail: rnzuckermann@lbl.gov

† Electronic supplementary information (ESI) available: Synthesis procedure for peptoid polymers; assembly conditions for nanosheet formation; mineralization procedures; additional AFM, TEM and electron diffraction data on mineralized nanosheets. See DOI: 10.1039/c5cc03323c

Recently, certain sequence-defined peptoid polymers have been discovered that self-assemble into highly stable two-dimensional nanosheets that are free-floating in water.[19] The nanosheets are bilayer structures, hundreds of micrometers in length and width, yet only 3 nm thick. The nanosheets can serve as 2D scaffolds with high surface area which can be readily functionalized to display a high density of molecular binding sites on both faces of the sheet.[20] Moreover, peptoid nanosheets are stable in air and in water at a variety of pH's, and do not aggregate in solution.[21] The peptoid nanosheet surface is hydrophilic and zwitterionic, which enables them to form stable free-floating suspensions in solution (Fig. S1, ESI†). Recently Olivier *et al.* demonstrated that peptoid nanosheets surface-functionalized with a gold binding peptide, effectively nucleated the growth of gold films on the sheet surface, suggesting that the nanosheets can serve as an effective platform for templating inorganic materials.[20] Natural $CaCO_3$ mineralization proteins are typically acidic, with a relatively large number of glutamic acid and aspartic acid residues.[18,22–25] Peptidomimetic oligomers bearing multiple acidic side chains have been shown to promote the nucleation of $CaCO_3$ crystal growth.[26–28] In fact, Chen *et al.* reported that short acidic peptoid oligomers can control the morphology of growing calcite crystals, and can even accelerate the crystal growth rate by a factor of >20-fold.[27,29] Thus, peptoid nanosheets are promising template as they display a high surface density of carboxylic acid groups, and can be synthesized in high yield. Furthermore, the nanosheets have a well-defined structure, which can be readily engineered at the atomic level, allowing precise tunability of the material properties.

Ultimately, we aim to produce peptoid-based nacre mimetics by layering individual, free floating planar composite units together into a bulk material (Fig. 1). Here, we focus on efficient methods to mineralize free-floating peptoid nanosheets with a controllable thickness of surface $CaCO_3$ films. Both the top and bottom solvent-accessible surfaces of the peptoid nanosheets are envisioned to provide a multivalent Ca^{2+} binding surface, and thus serve as a template to mineralize calcium carbonate.[30] There is precedent for similar materials that template the growth of amorphous calcium carbonate (ACC). For example, films of ACC were grown on planar zwitterionic lipid surfaces, which were subsequently converted into crystalline $CaCO_3$.[31] Carboxylic acid-rich polymers have been shown to stabilize a liquid-like precursor phase of calcium carbonate that can subsequently crystallize.[32] Two dimensional functional group arrays presented on self-assembled monolayers have also been shown to either stabilize ACC or promote its crystallization.[33] Thus it is reasonable to expect the peptoid nanosheet surface to serve as a substrate for ACC growth, and to potentially stabilize the ACC long enough to allow further assembly prior to crystallization.

Once a nanosheet is mineralized, it is essentially a single, free-standing lamellar composite planar building unit which can be further assembled into higher order structures. These single units or "nacre synthons" will be later stacked to form lamellar organic–inorganic multilayer composite structures. We anticipate the stacked ACC-covered peptoid nanosheets can be induced to crystallize into a layered brick-and-mortar architecture, to create a novel and structurally tunable organic–inorganic composite material. The nanosheet mineralization reactions performed here are *via* CO_2 diffusion into aqueous solutions containing $CaCl_2$ and peptoid nanosheets. The mineralization process was followed by scanning electron microscope (SEM), atomic force microscope (AFM), X-ray energy dispersive spectroscopy (EDS), and transmission electron microscopy (TEM).

We aimed to create $CaCO_3$ layers tens of nanometers thick on each side, in order to reach a final material composition of ~5% organic/95% inorganic (v/v), which is the approximate ratio found in nacre. We chose one of the most extensively studied nanosheets, made from a single peptoid 28 mer, called block-28 (B28), which consists of 14 ionic groups (seven *N*-(2-carboxyethyl)glycine and seven *N*-(2-aminoethyl)glycine monomers), alternating with 14 hydrophobic groups (*N*-(2-phenylethyl)glycine monomers) (Fig. 1a). Nanosheet assembly is achieved at pH 8, where the hydrophilic charged monomers become solvent-exposed and the hydrophobic monomers converge to form the hydrophobic core of the nanosheet bilayers.[20] Moreover, because the pI of a single B28 strand is 6.5,[20] the carboxylic acids moieties on the surface are expected to be largely deprotonated under the basic mineralization conditions, creating a net anionic sheet surface. First, the amphiphilic B28 peptoid was prepared as previously reported by the solid-phase submonomer method,[34] and purified to >95% purity by reverse phase HPLC. Peptoid nanosheets were then produced by the vial rocking method,[35] on a scale of 20 nmol followed by removal of free peptoid strands *via* spin filtration. Peptoid nanosheets were then mineralized with $CaCO_3$ by submerging the nanosheets in a 10 mM $CaCl_2$ solution and allowing CO_2 to diffuse in slowly (Fig. S2, ESI†). In order to keep the nanosheets at a defined position in the solution during mineralization, we used a 2% agarose gel (w/v) to support the nanosheets in solution. Mineralization was initiated by immersing the sheets in a 10 mM $CaCl_2$ solution and then exposing them to CO_2 in a closed chamber (*via* ammonium carbonate diffusion). After mineralization, the nanosheets were transferred to a silicon nitride substrate for further characterization *via* SEM, AFM, TEM and EDS analysis.

The presence of minerals on the nanosheet was confirmed by scanning electron microscopy (SEM). The morphology of individual nanosheets was examined after 3 hours. Compared to

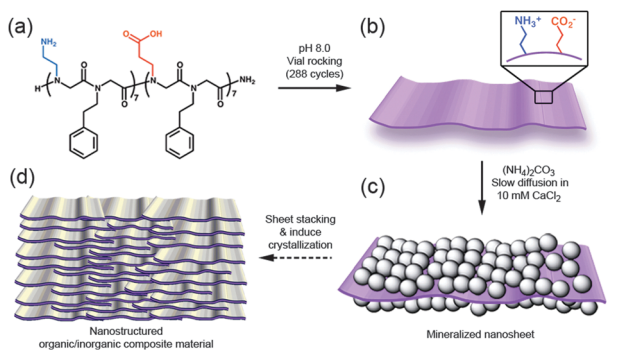

Fig. 1 Assembly pathway toward building peptoid-based nacre mimetic materials. (a) A sequence-defined amphiphilic peptoid chain (B28) is synthesized *via* solid-phase submonomer method, and (b) assembled into carboxylic rich peptoid nanosheets, which act as a template for ACC mineralization to produce (c) free-floating "nacre synthons." (d) These planar nacre synthons will be stacked to form brick-and-mortar, organic–inorganic nanocomposites.

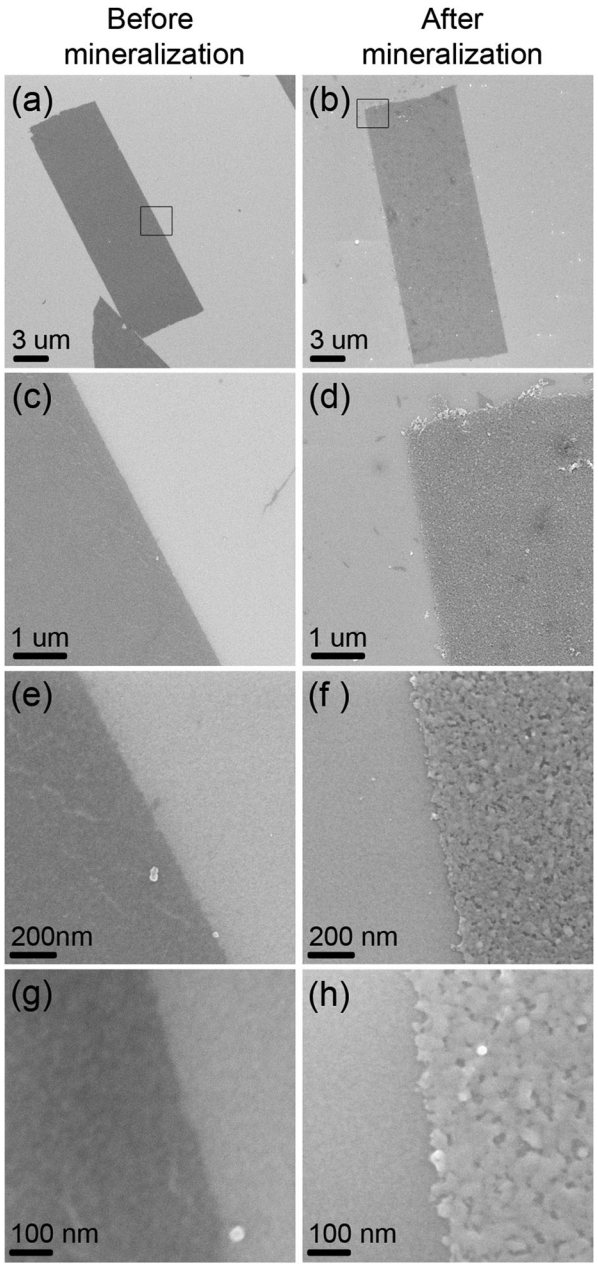

Fig. 2 Comparison of peptoid nanosheet morphology before and after mineralization as determined by SEM. (a), (c), (e), and (g) show the nanosheet before mineralization with increasing magnification, starting from the square box drawn in (a). (b), (d), (f), and (h) show the nanosheet after 3 hours of mineralization with increasing magnification starting from the square box drawn in (b).

un-mineralized peptoid nanosheets, the mineralized nanosheets looked much thicker and rougher, while retaining their straight edges and overall shape (Fig. 2). At high magnification, the mineralized sheet (Fig. 2h) shows a clear difference in the surface morphology as compared to un-mineralized sheets (Fig. 2g). SEM indicates a continuous film that has a high density of partially coalesced spherical features, similar to previously published reports on amorphous calcium carbonate.[36] No non-specific deposition of minerals was observed on the silicon nitride substrate surface indicating that the nanosheets can serve as a selective template for the growth of minerals. AFM can report on film thickness, and was thus used to investigate the growth kinetics of $CaCO_3$ on the peptoid template (Fig. 3). The un-mineralized B28 peptoid nanosheets have a thickness of approximately 3 nm according to both XRD and AFM.[19] Upon mineralization, the sheets gradually grew in thickness reaching a total thickness of $\sim$20 nm in 3 hours. Since both sides of sheet are mineralized, the mineralization growth rate on each surface was approximately 2–3 nm h^{-1}. Lastly, we studied the mineralized peptoid sheets through transmission electron microscopy. EDS spectra (Fig. 4a) clearly show presence of Ca, C and O only over the sheets. The diffraction pattern and the high resolution image show broad diffused rings (Fig. 4c) and lack of periodic features (Fig. 4e) respectively, a typical signature of an amorphous material. These results are consistent with an amorphous mineral layer covering the peptoid core. The mineralized sheet was found to be beam sensitive. When subjected to high electron dose ($>10^{10}$ e^- nm^{-2}) it transformed to a crystalline phase (yellow circles in Fig. 4b). High resolution imaging (Fig. 4d) reveals crystalline domains of a cubic nature with a typical 5–20 nm domain size. Electron diffraction of the irradiated material (Fig. 4f) can be indexed as the rock-salt crystal structure ($F3m$) of calcium oxide.[37] ACC has been shown to be a precursor to other crystalline phases of calcium carbonate.[38] However, when irradiated by a high dose of 200 keV electrons the ACC is

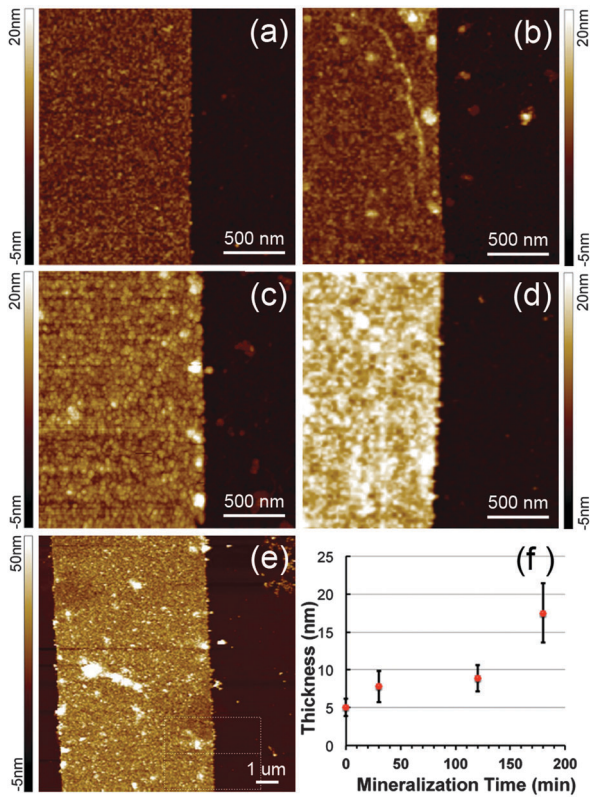

Fig. 3 The growth kinetics of $CaCO_3$ on the peptoid nanosheet was examined by measuring the thickness of multiple individual nanosheets at (a) 0 min, (b) 30 min, (c) 2 hours, and (d) 3 hours of mineralization by AFM. (e) Low magnification image of a mineralized nanosheet. (f) The increase in nanosheet thickness as a function of mineralization time, as determined by AFM.

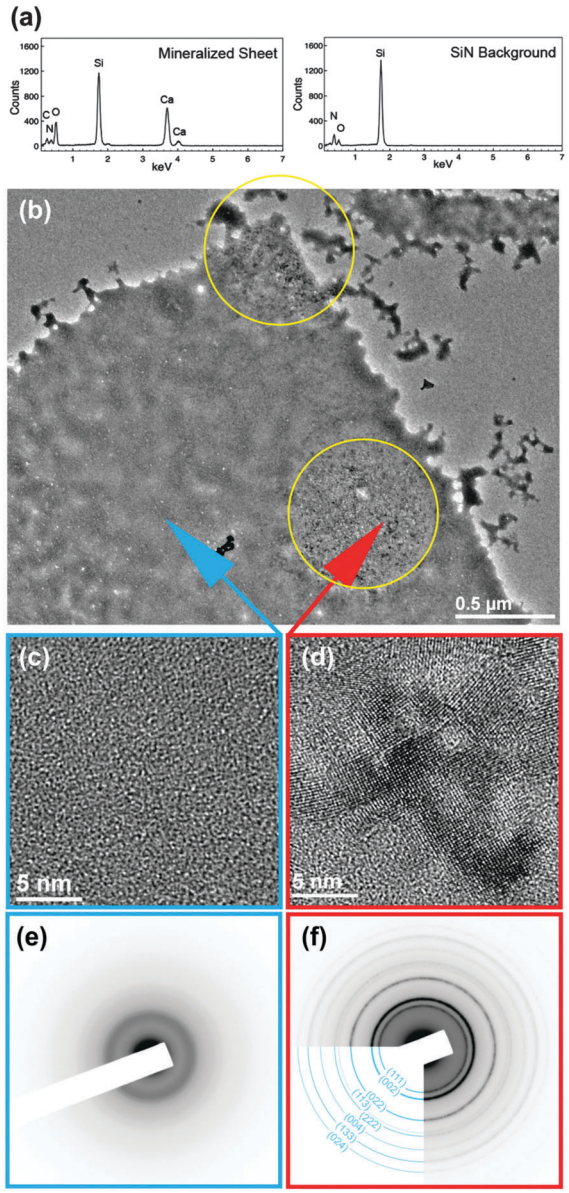

Fig. 4 TEM characterization of a mineralized peptoid nanosheet. (a) EDS spectra of mineralized sheet and Si_3N_4 support. (b) TEM image of the mineralized sheet. Yellow circles mark regions subjected to high dose electron irradiation ($\sim 10^{10}$ e^- nm^{-2}). High-resolution images (c and d), and diffraction patterns (e and f) of low-dose (c and e) and high-dose (d and f) irradiated areas.

dehydrated forming the more stable crystalline calcium oxide. The latter is a common form of $CaCO_3$ decomposition and has been observed to occur under electron irradiation.[39] The identification of CaO as decomposition product of the amorphous layer further confirms successful growth of ACC on the peptoid sheets.

We successfully developed an efficient strategy for ACC growth on peptoid nanosheets in solution. Using a simple CO_2 diffusion method to mineralize nanosheets, we obtained peptoid nacre synthons that have approximately 10 nm layers of ACC on each face. The composition, morphology and identity of the ACC film were confirmed by AFM, SEM, TEM and EDS. We believe that the experimental methodology developed in this work can provide unique building blocks for constructing artificial nacre materials, as these nanoscale synthons are prepared in solution, and can be readily scaled up. In the future, we plan to stack these nacre mimetic peptoid synthons to synthesize brick-and-mortar architecture and study their mechanical properties.

This project was funded by the Defense Threat Reduction Agency under Contract No. DTRA10027-15875. The work was conducted at the Molecular Foundry at Lawrence Berkeley National Laboratory, which is supported by the Office of Science, Office of Basic Energy Sciences, U. S. Department of Energy, under Contract No. DE-AC02-05CH11231.

Notes and references

1 L. Addadi and S. Weiner, *Nature*, 1997, **389**, 912.
2 S. Mann, *Biomineralization: Principles and concepts in Bioinorganic Materials Chemistry*, Oxford University Press, Oxford, 2001.
3 J. Wang, Q. Cheng and Z. Tang, *Chem. Soc. Rev.*, 2012, **41**, 1111.
4 J. Sun and B. Bhushan, *RSC Adv.*, 2012, **2**, 7617.
5 A. Walther, I. Bjurhager, J.-M. Malho, J. Pere, J. Ruokolainen, L. A. Berglund and O. Ikkala, *Nano Lett.*, 2010, **10**, 2742.
6 R. O. Ritchie, *Nat. Mater.*, 2014, **13**, 435.
7 N. Hosoda, A. Sugawara and T. Kato, *Macromolecules*, 2003, **36**, 6449–6452.
8 I. A. Aksay, M. Trau, S. Manne, I. Honma, N. Yao, L. Zhou, P. Fenter, P. M. Eisenberger and S. M. Gruner, *Science*, 1996, **273**, 892.
9 R. O. Ritchie, *Nat. Mater.*, 2011, **10**, 817.
10 B. R. Heywood and S. Mann, *Adv. Mater.*, 1994, **6**, 9.
11 E. R. Kleinfeld and G. S. Ferguson, *Science*, 1994, **265**, 370–373.
12 P. Podsiadlo, S. Paternel, J.-M. Rouillard, Z. Zhang, J. Lee, J.-W. Lee, E. Gulari and N. A. Kotov, *Langmuir*, 2005, **21**, 11915.
13 S. Deville, E. Saiz, R. K. Nalla and A. P. Tomsia, *Science*, 2006, **311**, 515.
14 A. Sellinger, P. M. Weiss, A. Nguyen, Y. Lu, R. A. Assink, W. Gong and C. J. Brinker, *Nature*, 1998, **394**, 256.
15 Z. Tang, N. A. Kotov, S. Magonov and B. Ozturk, *Nat. Mater.*, 2003, **2**, 413.
16 P. C. A. Finnemore, T. Shean, S. Vignolini, S. Guldin, M. Oyen and U. Steiner, *Nat. Commun.*, 2012, **3**, 966.
17 Y. Wang, A. S. Angelatos and F. Caruso, *Chem. Mater.*, 2007, **20**, 848.
18 C.-A. Wang, B. Long, W. Lin, Y. Huang and J. Sun, *J. Mater. Res.*, 2008, **23**, 1706.
19 K. T. Nam, S. A. Shelby, P. H. Choi, A. B. Marciel, R. Chen, L. Tan, T. K. Chu, R. A. Mesch, B.-C. Lee, M. D. Connolly, C. Kisielowski and R. N. Zuckermann, *Nat. Mater.*, 2010, **9**, 454.
20 G. K. Olivier, A. Cho, B. Sanii, M. D. Connolly, H. Tran and R. N. Zuckermann, *ACS Nano*, 2013, **7**, 9276.
21 R. Kudirka, H. Tran, B. Sanii, K. T. Nam, P. H. Choi, N. Venkateswaran, R. Chen, S. Whitelam and R. N. Zuckermann, *Pept. Sci.*, 2011, **96**, 586.
22 F. Jones and M. I. Ogden, *CrystEngComm*, 2010, **12**, 1016.
23 N. A. J. M. Sommerdijk and G. D. With, *Chem. Rev.*, 2008, **108**, 4499.
24 A.-W. Xu, Y. Ma and H. Colfen, *J. Mater. Chem.*, 2007, **17**, 415.
25 L. Addadi and S. Weiner, *Proc. Natl. Acad. Sci. U. S. A.*, 1985, **82**, 4110.
26 L. A. Estroff, C. D. Incarvito and A. D. Hamilton, *J. Am. Chem. Soc.*, 2004, **126**, 2.
27 C.-L. Chen, J. Qi, J. Tao, R. N. Zuckermann and J. J. DeYoreo, *Sci. Rep.*, 2014, **4**, 6266.
28 J. J. J. M. Donners, R. J. M. Nolte and N. A. J. M. Sommerdijk, *J. Am. Chem. Soc.*, 2002, **124**, 9700.
29 C.-L. Chen, J. Qi, R. N. Zuckermann and J. J. DeYoreo, *J. Am. Chem. Soc.*, 2011, **133**, 5214.
30 L. Addadi and S. Weiner, *Angew. Chem., Int. Ed.*, 1992, **31**, 153.
31 J. Xiao, Z. Wang, Y. Tang and S. Yang, *Langmuir*, 2009, **26**, 4977.
32 L. B. Gower and D. J. Odom, *J. Cryst. Growth*, 2000, **210**, 719.
33 T. Y.-J. Han and J. Aizenberg, *Chem. Mater.*, 2007, **20**, 1064.
34 H. Tran, S. L. Gael, M. D. Connolly and R. N. Zuckermann, *J. Visualized Exp.*, 2011, **57**, e3373.
35 B. Sanii, R. Kudirka, A. Cho, N. Venkateswaran, G. K. Olivier, A. M. Olson, H. Tran, R. M. Harada, L. Tan and R. N. Zuckermann, *J. Am. Chem. Soc.*, 2011, **133**, 20808.
36 Y. Liu, Y. Cui and R. Guo, *Langmuir*, 2012, **28**, 6097.
37 R. W. G. Wyckoff, *Crystal Structures*, Interscience, New York, 2nd edn, 1963.
38 L. Addadi, D. Joester, F. Nudelman and S. Weiner, *Chem. – Eur. J.*, 2006, **12**, 980.
39 K. M. Towe, *Nature*, 1978, **274**, 239.